Shock metamorphism of olivine in NWA 1950 lherzolitic shergottite. A. Takenouchi, T. Mikouchi, T. Kogure, S. Inoue, Department of Earth and Planetary Science, The University of Tokyo, 7-3-1 Hongo, Bunkyo-ku, Tokyo 113-0033, Japan.

Introduction:

Most Martian meteorites are metamorphosed by heavy shock, which causes undulose extinction of olivine and pyroxene, transformation of plagioclase into diaplectic glass ("maskelynite"), formation of shock melts and darkening of olivine crystals ("brown" olivine). [1,2] first performed detailed TEM studies of brown olivine by the discovery of NWA2737 chassignite, and they found iron nano-particles in olivine as well as changes of reflection spectra and magnetic characteristics. They concluded that brown color of olivine is due to the formation of these iron nano-particles. Although these nano-particles are considered to form by the shock effect, their formation process is not well understood.

The presence of brown olivine is a unique feature of Martian meteorites, which may reflect specific condition of shock events on Mars. Therefore, we performed a detailed study of brown olivine in a Martian meteorite to better understand planetary shock events and to reveal the singularities of Martian meteorites.

Sample and Method:

In this study we analyzed Northwest Africa 1950 (NWA 1950) which is classified into lherzolitic shergottite and mainly consists of olivine, pyroxene and maskelynite [3,4]. Most olivine grains in this meteorite are colored and the previous studies found two different species of iron nano-particles, which are iron metal and magnetite [2,5]. We specially selected NWA 1950 because no other Martian meteorites are known to contain two different species of nano-particles, which may have substantial information about the formation of iron nano-particles in olivine.

We first analyzed thin sections by optical microscopy, FEG-SEM (Hitachi S-4500) with EBSD detector and EPMA (JEOL JXA8530F). TEM foil was extracted from the thin section by FIB (Hitachi FIB 2100) and also a powder sample with brown olivine was prepared. These TEM samples were observed by TEM (JEOL JEM-2010) and HAADF-STEM (JEOL JEM-2800) (high-angle annular dark field scanning transmission electron microscopy). Micro-Raman analysis (JASCO NRS-1000) was also applied for the phase identification.

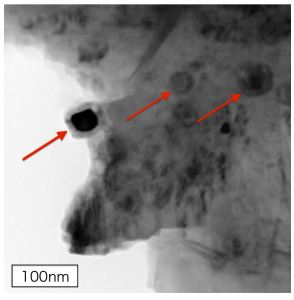

Fig. 1. Iron metal nano-particle mantled by magnetite (indicated by red arrows)

Result:

The observation of the TEM powder sample reveals that brown olivine contains abundant iron nano-particles ("ordinary" nano-particles) whose sizes are 5~100 nm. This size range is slightly wider than that previously reported in NWA 2737 (5~20 nm) [1]. Electron diffraction patterns of iron nano-particles show that all particles in this sample are iron metal and there are no magnetite particles. However, there are rare iron metal nano-particles that are mantled by thin magnetite rims (Fig. 1). This texture was not reported before.

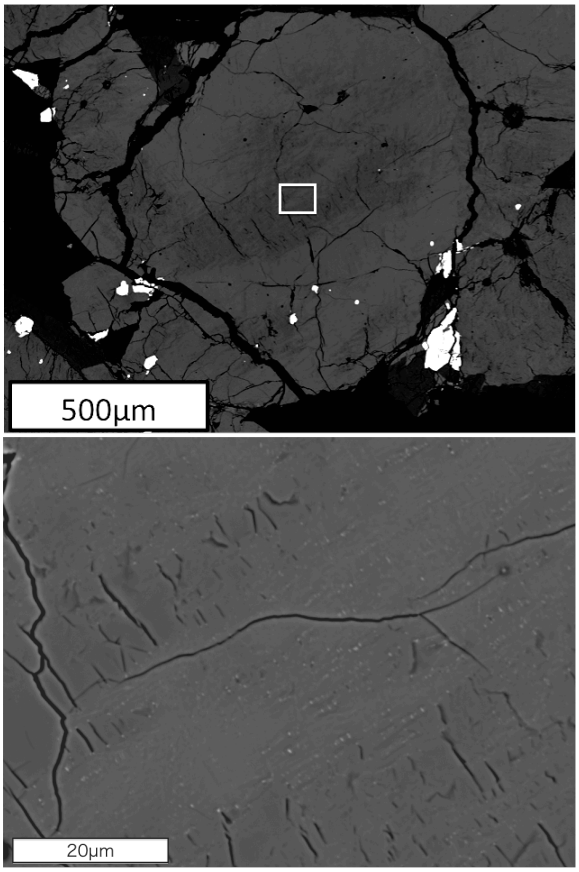

Fig. 2. Back-scattered electron (BSE) images of colored olivine. Upper image shows a whole colored olivine grain and the bottom one shows enlarged portion indicated in the upper image.

As mentioned above, most olivine grains in NWA 1950 are colored and show undulose extinction under transmitted light of optical microscopy. The degree of coloration shows variation from one domain to another. The SEM observation by BSE imaging shows that the colored domains are slightly brighter than the non-colored ones (Fig. 2) and the former has less cracks than the latter. EBSD analysis reveals that the colored (brighter) domains have poorer crystallinity than the other ones. Although there are such differences between these different domains, they have almost

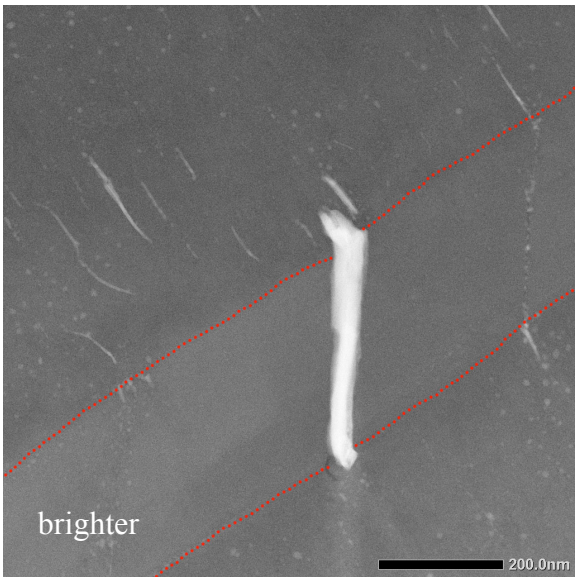

Fig. 3. HAADF-STEM image of band-like area with iron grains.

identical chemical compositions. [1] reported that olivine in NWA2737 is also composed of two kinds of domains with different contrast in BSE images like the one in NWA1950 and they concluded that these domains were dense polymorphs of olivine. However in this study, their Kikuchi-patterns proved that they have the same crystal structure as that of olivine.

FEG-SEM observation with high magnification and high electron current reveals that there are iron submicron-sized grains in the colored (brighter) domains (Fig. 2). These grains are arranged in a band-like area with brighter BSE contrast that extends along a certain crystallographic plane of the host olivine crystal. These areas were extracted by FIB and observed by HAADF-STEM. The HAADF image reveals that the band-like area obliquely penetrates into the domain (from left bottom to right middle of Fig. 3). This band-like area is slightly more Fe-rich than the outside of the area, while there is no distinct difference in the Si content. In addition, the band-like area appears smoother in TEM images and this indicates that the area has less defects than the outside.

Around the band-like area, there are "ordinary" iron nano-particles, and also rod-like iron metals are present. However, there are less abundant iron nano-particles inside the area. The brightest grain at the near center of the image (Fig. 3), which is a kindred grain in the BSE images (submicron-sized grains), is iron metal and tilted observation shows that it is a thin film-like shape. Such iron metals are arranged in the banded areas at irregular intervals and some of them are not filmy, but aggregates of nano-particles along a plane parallel to the films. Similar to this, there are a wide variety of iron particles in the colored olivine.

There is a thin shock melt vein (50 μm wide) adjacent to olivine. This olivine grain is bright in BSE image near the contact with shock melt. These zones show a similar texture to polycrystalline ringwoodite reported in L6 chondrites [6]. However, micro-Raman analysis shows that they are not ringwoodite but olivine. [4] reported stishovite and wadsleyite in NWA 1950, but we have not found any high-pressure minerals (especially, ringwoodite) in our samples so far.

Discussion and Conclusion:

This study exhibits some clues to elucidate the mechanism of olivine darkening and the formation of iron particles in olivine. First, the colored olivine domains seem to be annealed (not totally molten) because the number of cracks is less than that in the colorless domains. If they were molten, all iron metal particles would be the same shapes and differences of olivine compositions may arise. We consider the formation of iron particles without melting by the following reasons. Paying attention to rod-like iron particles, their iron contents seem to be reduced from olivine and concentrate by diffusion along defects such as dislocations. The reduction may occur at high temperature under a certain oxygen fugacity (most iron particles were formed during this time) and subsequently an oxidation may occur after the temperature dropped. This redox change accompanying the temperature change results in the formation of iron nano-particles mantled by magnetite. As for the iron films, they appear to be formed under shear stresses. However, further investigation is required to reveal their formation process.

In olivine adjacent to the shock melt vein, we found a ringwoodite pseudo-structure. This indicates olivine zones around shock melt experienced extremely high temperature and pressure, and once transformed into ringwoodite, but they retrograded because the temperature drop was too slow for them to survive. This may be caused by the high temperature throughout the whole meteorite resulted from extensive post-shock heating. On the other hand, persistence of high temperature formed iron nano-particles by Fe diffusion in olivine. These thermal and pressure histories may be unique to Martian meteorites containing brown olivine. In order to support this hypothesis, more observation of other Martian meteorites and comparison to other shocked meteorites are required, and now they are in progress.

References:

[1] Treiman, A. H. et al., (2007) *JGR, 112, E04002.* [2] Van de Moortèle, B. et al., (2007) *EPSL, 262, 37-49.* [3] Mikouchi, T., (2005) *Meteorit. Planet. Sci., 40, 1621-1634.* [4] Gillet, P. et al., (2005) *Meteorit. Planet. Sci., 40, 1175-1184.* [5] Kurihara T. et al. (2009) LPS XL, abst. #1049. [6] Miyahara M. et al., (2010) *EPSL, 295, 321-327.*